

# MobiCom: G: Battery-free Visible Light Sensing

Andreas Soleiman

Advisor: Ambuj Varshney

Uppsala University, Sweden

andreas.soleiman@it.uu.se

## ABSTRACT

We present the first visible light sensing system that can sense and communicate shadow events while only consuming tens of  $\mu\text{W}$ s of power. Our system requires no modification to the existing lighting infrastructure and can use unmodulated ambient light as a sensing medium. We achieve this by designing a sensing mechanism that utilizes solar cells, and an ultra-low power backscatter based transmission mechanism we call *Scatterlight*, which can communicate sensor readings without the use of any energy-expensive computational block. Our results demonstrate the ability to sense and communicate various hand gestures at peak power consumption of tens of  $\mu\text{W}$ s at the sensor, which represents orders of magnitude improvement over the state-of-the-art.

## 1 INTRODUCTION

Visible light is a ubiquitous medium that can provide illumination to spaces or objects by natural light or through artificial light sources such as fluorescent bulbs or light emitting diodes (LEDs). It can be sensed using simple and inexpensive photodiodes or solar cells which require minimal processing effort at the sensing device. Thus, visible light offers a significant advantage over mediums such as radio frequency (RF), which require complex signal processing at reception. Further, RF based sensing applications suffer from cross-technology interference (CTI) due to an increased amount of devices sharing the same regulated spectrum. In comparison, visible light exists in an unregulated spectrum, and its directional nature allows for alteration of the medium in more confined spaces.

However, despite the clear advantages of visible light over RF for sensing applications, there have only been limited deployments of visible light sensing (VLS) systems (excluding vision-based systems). One of the reasons for the lack of pervasive deployment of VLS systems is that a majority of existing systems fail to take advantage of the ubiquitous nature of visible light, since they modify the existing lighting infrastructure to enable visible light communication (VLC). VLC requires retrofitting of luminaries with specialized driving circuits [3–5] to modulate visible light, with e.g. beacon information. Modifying existing lighting infrastructure significantly increases the cost and complexity of deployment [14]. Moreover, existing VLC systems use complex reception logic and circuitry to perform demodulation [3], or FFT operations [4, 5] which further hinders pervasive deployment of VLS systems. Thus, a key enabler to achieve widespread deployment of VLS systems is to use unmodulated ambient light for sensing.

The use of unmodulated ambient light for sensing allows for tracking shadows cast by objects or people. Recent efforts show that sensing changes in the cast shadow enables human sensing capability [4, 5], or tracking of hand gestures [6]. However, several



**Figure 1: Shadow sensing at  $\mu\text{W}$ s of power. We can detect and communicate shadow events by reflecting ambient RF signals while consuming 20  $\mu\text{W}$ s of power.**

limitations remain that hinder widespread deployment: *First*, some prior shadow sensing systems use modulated light [4, 5] which, as discussed above, makes the deployment complex. *Second*, these systems [4–6] employ conventional light sensing mechanisms.

Conventional light sensing mechanisms [4–6] employ sensors with components that negatively affect pervasive deployment: they amplify the signals from photodiodes using transimpedance amplifiers (TIAs), sample using analog to digital converters (ADCs), and process using computational blocks involving microcontrollers (MCUs) or field-programmable gate arrays (FPGAs). Further, the events are communicated using traditional RF radios [1] or external cables [4, 5]. There are three main problems with this approach: *First*, it consumes significant amounts of power (mWs) and hence requires sensors that are battery-powered or powered through other external sources. *Second*, TIAs suffer from saturation under bright light conditions [6] which prevents continuous operation under natural and ambient light. *Finally*, all of these components significantly increase the cost of sensors, which makes it challenging and expensive to deploy the system at scale.

**Contributions.** We present our vision to design simple and low cost and power light sensors with the ability to sense changes in ambient light. Such sensors can operate on small amounts of energy harvested from ambient light and transform any well-lit surface to a sensing medium. The combination of simple, inexpensive, and ultra-low power sensors could make VLS systems pervasive. To enable our vision, we use unmodulated light to sense shadows by building on recent systems [4, 5].

We introduce the first VLS system that can sense changes in unmodulated ambient light by tracking shadows, and communicate these events while consuming tens of  $\mu\text{W}$ s of power. To achieve this, we make two key contributions over existing state-of-the-art systems [4, 5]: *First*, we overcome the high power consumption for sensing by using solar cells as light sensors. Unlike photodiodes which require energy-expensive TIAs for operation, solar cells are passive, can harvest energy, and can operate under diverse light conditions without being affected by saturation. *Second*, we overcome the overhead of communicating sensor readings by using RF backscatter. We embrace a key observation by Zhang et al. that local processing at the sensing device is significantly more

energy-expensive than backscatter transmissions [15]. We devise a mechanism called *Scatterlight*, which offloads sensor readings to powerful end-devices without performing any local processing. This allows for ultra-low power and inexpensive sensors, which we call visible light markers (VLMs). The resulting system is illustrated in Figure 1. It consists of a carrier signal source, a VLM, and a device to receive and process the backscattered signals.

## 2 RELATED WORK

Our work is related to the following:

**Shadow sensing.** Prior work has explored shadow sensing. Li et al.’s system uses an array of photodiodes deployed on the floor together with modulated lights to track user gestures [4, 5]. In a more recent work, Li et al. detect hand gestures by tracking changes in light levels caused by hand motions above multiple photodiodes under unmodulated ambient light [6]. However, all of the above systems used conventional light sensing mechanisms which involves photodiodes coupled with TIAs, and ADCs for sampling on COTS platforms (Arduinos). These mechanisms are energy expensive (mW), and are susceptible to saturation under bright light.

**Solar cells as light sensors.** Solar cells as light sensors have been restricted to high-speed VLC systems. For example, Wang et al. use a solar panel as a light sensor coupled to an energy-expensive voltage amplifier and ADCs, and receive using a complex OFDM modulation scheme [13]. However, these designs are not suited for battery-free systems due to their high power consumption.

**Unmodulated ambient light for sensing.** Zhang et al. [16] and Shu et al. [17] demonstrate that indoor lights exhibit a characteristic frequency which enables indoor localization applications. These systems are similar to our system in terms of using unmodulated light and require no infrastructure modifications. However, they use smartphones for sensing which consumes mWs of power.

**Processing overhead.** Prior attempts [10, 15] have investigated the processing overhead on backscatter sensors. Zhang et al. optimise the computational block, and demonstrate that processing is more energy expensive than backscatter transmissions. Talla et al. [10], in a concurrently released work, design a battery-free cellphone. Their design is similar to *Scatterlight* in terms of eliminating computational blocks. However, we make significant improvements over their design: Talla et al. backscatter at the same frequency as the carrier signal and thus encounter severe self-interference [16]. In comparison, *Scatterlight* without involving computation blocks can also shift the backscatter signal away from the carrier, thereby significantly reducing self-interference. Finally, concurrent to our efforts, Naderiparizi et al. [8] devise an analog backscatter technique that eliminates computational blocks and enables battery-free HD video streaming.

## 3 DESIGN

### 3.1 Overview

The fundamental operation of our system is to detect and transmit changes in ambient light caused by shadows. We base our design of the VLM on mitigating the key bottlenecks of state-of-the-art VLS systems; high power consumption (mW) due to conventional

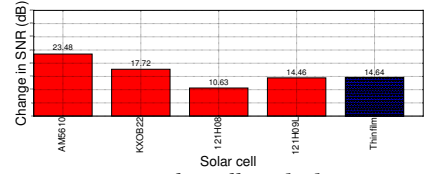


Figure 2: Sensing using a solar cell. A shadow cast on a solar cell causes a significant change in the SNR.

sensing mechanisms, local processing and energy cost for communication, as well as the complexity of deployment. To achieve this, our system performs a series of steps, as we describe next.

First, we generate a carrier signal so that the VLM can backscatter shadow events. We provide a brief introduction to RF backscatter in section 3.2. Next, in section 3.3, we describe the use of solar cells to sense shadow events at ultra-low power consumption. Further, we discuss our contribution *Scatterlight*, avoids computational blocks by offloading sensor readings to an end device through backscatter communication. We design two version of VLMs that support different sensing resolution depending on the application scenario. Our first design couples a solar cell to a thresholding circuit to digitize sensor readings and communicate them using the Scatterlight mechanism. We call this design thresholding VLM (tVLM). Our second design, at the expense of slightly higher energy consumption, directly transmits the solar cell output without digitization, and supports a higher resolution. We call this design analog VLM (aVLM).

### 3.2 Ambient RF signal

To enable ultra-low power communication of shadow events, we utilize RF backscatter. By using RF backscatter, we avoid the energy-expensive operation of generating a modulated RF signal at the sensing device to communicate the desired information. Instead, we can communicate by reflecting ambient RF signals.

### 3.3 Visible Light Marker

In this section, we present the design choices for our VLMs, which enable ultra-low power sensing and communication.

**Solar cells as light sensors.** To decrease the power consumption for visible-light sensing to  $\mu$ Ws which is necessary for battery-free operation, we take advantage of solar cells to achieve the necessary amplification without energy-expensive amplifiers. Similar to photodiodes, solar cells transform variations in ambient light caused by, e.g., a shadow to a change in the electrical signal. Solar cells have been recently used to enable high-speed VLC using energy-hungry ADCs [13]. To the best of our knowledge, solar cells have not been explored for VLS.

**Selecting solar cell for sensing.** We evaluate six different commercial solar cells of different characteristics to select the one that is most responsive to sensing a shadow. We place a solar cell on the floor, and cast a shadow on it. We track its analog output using a logic analyser. We perform the experiment three times for each solar cell. Figure 6 demonstrates that all six solar cells observe a significant change ( $> 10$  dB) in the signal-to-noise ratio (SNR) which confirms that solar cells can be used for passive sensing. Among the best performing solar cells, the thinfilm solar cell offers the highest short-circuit current which improves energy harvesting performance. Thus, we select the thin film (USD 4) solar cell.

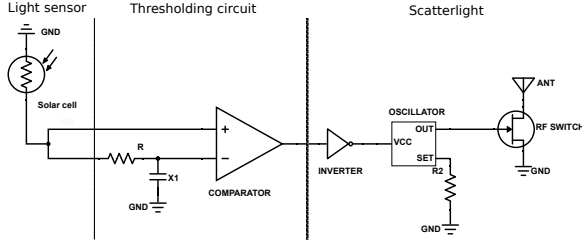


**Figure 3: Thresholding Visible Light Marker (tVLM) schematic.** tVLM senses and digitizes shadow events at sub- $\mu\text{W}$  of power. Further, it communicates the events without performing local processing at a peak power of  $20\ \mu\text{W}$ .

**Eliminating computational blocks.** A key bottleneck on existing sensors is the high energy consumption for the computational blocks involved [10, 15]. On existing sensing systems, processing the analog signals and converting them to the digital domain contributes significantly to the high energy consumption. Existing VLS systems use energy expensive platforms such as Arduinos with ADCs to preprocess light samples and transfer these to an end-device such as a workstation [4, 5]. Keeping these challenges in mind, we ask ourselves the question: *how can we eliminate the computational blocks and communicate the sensor data while consuming tens of  $\mu\text{W}$ s at the sensing device?* We address these challenges next through the Scatterlight mechanism.

**Scatterlight.** We eliminate the overhead of any power-hungry computational blocks such as an FPGA or an MCU by building on the observation by Zhang et al. [15] that processing is significantly more energy expensive than backscatter transmissions. We devise a mechanism we call *Scatterlight* which causes changes in backscattered signals as a function of either the digitized signals through the thresholding visible light marker (tVLM), or the analog sensor readings through analog visible light marker (aVLM). We face two main challenges to realise this concept: *First*, the carrier adds significant interference to the weak backscatter signals. *Second*, we have to modulate the carrier signal with shadow events without using computational blocks.

We solve the first challenge by building on recent systems [2, 16] that keep the backscattered and the carrier signal at separate frequencies: If the carrier signal is present at a center frequency  $f_c$ , while a VLM backscatters at a frequency  $\Delta f$ , the backscattered signal appears at an offset  $\Delta f$  away from  $f_c$ . This displacement reduces interference from the carrier [2, 12, 16], and allows the receiver to detect backscattered signals. A crucial question is the choice of  $\Delta f$ , which is transceiver dependent. We employ a transceiver that requires a  $\Delta f$  of at least 100 kHz [12].

Next, we describe how we overcome the second challenge, and realise the designs of the VLMs.

**Thresholding Visible Light Marker.** In the tVLM design, we employ a thresholding circuit in place of commonly employed ADCs to convert changes in analog signals to digitised values. A thresholding circuit, as shown in Figure 3 consists of a comparator and a low pass filter (LPF) composed of a resistor (R) and a capacitor (X1). The thresholding circuit acts like a 1-bit ADC, and gives a binary output indicating the absence or the presence of the shadow. The thresholding circuit tradeoffs sensing resolution for ultra-low power consumption, and enables us to achieve  $0.5\ \mu\text{W}$ s of power for

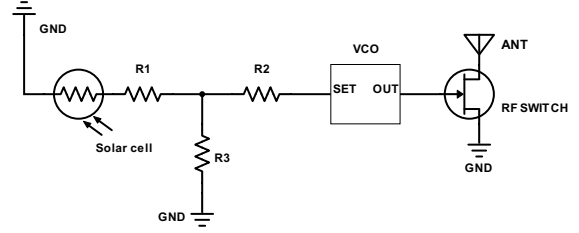


**Figure 4: Analog Visible Light Marker (aVLM) schematic.** Unlike tVLM, aVLM avoids digitization and communicates raw sensor data by mapping the sensor readings to different shifts in the frequency of the backscattered signal. The aVLM tradeoffs power consumption for sensing resolution; it operates at a peak power of  $120\ \mu\text{W}$ .

sensing and digitising changes in the ambient light levels. Thresholding circuits are commonly employed in backscatter systems [7]. However, to the best of our knowledge, we are the *first* to use a thresholding circuit with a solar cell for ultra-low power VLS.

Next, to transmit digitised sensor readings without computational blocks, we observe that a commodity radio transceiver or an SDR can enable fast sampling of RF signals. If we can backscatter for the duration of the shadow event, the presence and the duration of the shadow event can be determined at the receiver by sampling of the received backscattered signals. In tVLM, the thresholding circuit controls an ultra-low power oscillator (LTC 6906, USD 1.5) which in turn controls a backscatter switch (NXP BFT25A, USD 0.2), as shown in Figure 3. We configure the oscillator to a frequency larger than  $\Delta f$  required to mitigate self-interference. Hence, when there is a shadow event, the thresholding circuit enables the oscillator to generate a backscatter signal at a frequency  $\Delta f$  from the center frequency  $f_c$  of the carrier signal.

**Analog Visible Light Marker.** The tVLM tradeoffs sensing resolution (1-bit) for ultra-low power consumption, and achieves a peak power consumption of  $20\ \mu\text{W}$ s for its operation. tVLM can enable several VLS scenarios as we discuss in the evaluation section, however, the limited resolution can be restrictive for some application scenarios. To support VLS applications that require a higher sensing resolution, we tradeoff the power consumption in scatterlight and design aVLM.

aVLM is based on the following idea: if the backscattered signal appears at a frequency offset of  $\Delta f(V)$  away from  $f_c$ , where  $V$  is the output voltage from the solar cell, then, by tuning in to a frequency  $f_b(V_i) = f_c \pm \Delta f(V_i)$  at the receiver, we can detect the presence or the absence of the backscattered signal, and hence determine the sensor readings from the solar cell by mapping the received frequencies to voltages. To design aVLM, we eliminate the thresholding circuit, and instead feed the output of the solar cell to the oscillator acting as a voltage controlled oscillator (VCO). A VCO maps the input voltage to corresponding output frequency ( $\Delta f$ ) which can be set between between 100 kHz to 1 MHz, which defines the bandwidth for  $\Delta f(V_i)$ , i.e. 900 kHz. The higher bandwidth increases the power consumption of aVLM when compared to tVLM. We show the schematic of aVLM in the Figure 4, the solar cell controls the input voltage of the VCO, and the output frequency of the VCO controls the backscatter switch.

**Sensing Resolution of aVLM.** We define the sensing resolution of the aVLM, as the number of analog sensor readings that can be

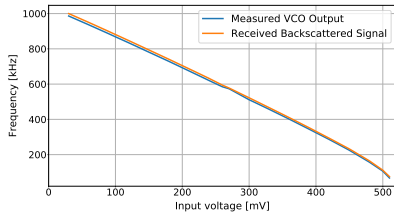


**Figure 5: Accuracy of detecting analog backscatter signals.** We observe that the maximum difference in frequency between the received backscatter signal and the VCO output frequency is 14 kHz.

detected at the receiver. The sensing resolution is analogous to the resolution of an ADC used in VLS systems. Since the aVLM maps analog sensor readings to frequency shifts of backscatter signals, its resolution, is defined as the number of *different* frequency shifts that can be detected at the receiver. The upper and lower bounds of these frequency shifts are determined by the frequency range of the VCO, i.e. 100 kHz to 1 MHz. However, since the VCO has an output frequency error, and the transmitting and receiving SDRs induce additional frequency errors, we are forced to correct for this by defining a constraint on how close we can separate the backscatter signals to be able to properly reconstruct the analog signal.

We define a *bin* as the minimum frequency-spacing that can be achieved, and the total number of bins within the frequency range of the VCO represents the maximum achievable sensing resolution of the aVLM. To compute a theoretical value for the resolution, we make the assumption that the frequency-to-voltage mapping is linear, as specified in the datasheet of the VCO, and that we have a frequency bandwidth of 900 kHz. Thus, the bit-resolution with an unknown minimum bin-spacing,  $x$ , is defined as follows

$$\log_2 \left( \frac{900}{x} + 1 \right), \quad x > 0. \quad (1)$$

We note that the LTC6906 has a maximum frequency output error of 0.5%, which means that the output frequency of the VCO (between 100 kHz to 1 MHz) results in a frequency error between  $\pm 500$  Hz to  $\pm 5$  kHz [11]. Further, the two SDRs induce an additional frequency error of  $\pm 2$  ppm per SDR [9]. Thus, at 2.48 GHz, we expect the frequency error from the SDRs to be close to  $\pm 10$  kHz. In total, by adding the absolute values of these frequency errors, we get a minimum bin-spacing between  $x = 10.5$  kHz to  $x = 15$  kHz. Using equation 1, we get a mean sensing resolution corresponding to 6-bits for aVLM.

**Translating Frequency Shifts to Sensor Readings.** At the receiver for aVLM, we have to perform an operation to map the frequency shifts to corresponding voltage to recover light sensor readings. This requires us to obtain the mapping function to perform this operation. Next, we perform an experiment to obtain this function: We fix the aVLM backscatter tag 1 m away from the carrier generator and we place the receiver 3 m away from the tag. Next, we connect the VCO to a programmable voltage source, and vary the input voltages to the VCO in 24 steps between 30 mV and 510 mV, while keeping track of its output frequency using a logic analyzer. At the receiver (SDR), we run a processing algorithm that performs FFT, signal smoothing using a moving average filter, and peak detection to extract the backscatter signals. We determine

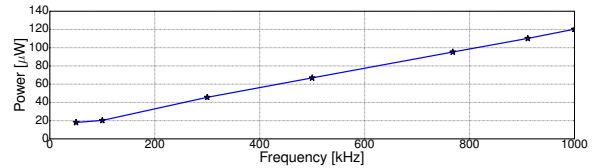


**Figure 6: Power consumption for tVLM at 2 V.** At a 100 kHz transmission frequency, the peak power consumption of tVLM is 20  $\mu$ W.

**Table 1: Power consumption breakdown for different components of VLMs at an operating voltage of 2 V.**

Module	Power consumption
Solar cell	0
Thresholding circuit	0.5 $\mu$ W
Scatterlight (tVLM, 100 kHz)	19.5 $\mu$ W
Scatterlight (aVLM, 1 MHz)	120 $\mu$ W

the instantaneous frequency shift  $\Delta f$  at the receiver by the simple equation:  $\Delta f = |f_c - f_r|$ , where  $f_c$  is the known carrier frequency and  $f_r$  is the received frequency.

Figure 5 demonstrates the result of the experiment, we approximate a linear fit between the input voltage to the VCO and the received backscatter signal frequency shift,  $\Delta f(V)$ . This gives us the following mapping function:

$$V = -0.534 \cdot \Delta f(V) + 56.804, \quad (2)$$

where  $V$  is the voltage control input to the VCO.

## 4 EVALUATION

In this section, we present our preliminary result to evaluate different aspects of our system. We perform experiment in range of different environment and conditions.

**Experiment setup.** We evaluate our system indoors under office lights which were 200 lx; a level much lower than typical indoor illumination. As an energy harvester, we use the TI BQ25570 since it can operate at very low input voltages. We use a capacitor of size 22  $\mu$ F that is comparable to other energy harvesting platforms such as CRFIDs. We use a thin film solar cell for both sensing and harvesting. At the VLM, we keep track of the analog signal from the solar cell, and the output of the thresholding circuit.

We use the test mode available on transceivers to generate carrier signals [12]. We generate each of these carrier signals at 868 MHz and 2.48 GHz, of strengths 24 dBm and 0 dBm, respectively. We use a TI CC1310 transceiver to generate the 868 MHz carrier, and a USRP-B200 software defined radio (SDR) to generate the 2.48 GHz carrier signal.

**Power consumption.** To measure the power consumption, we first connect a VLM in series with a Fluke multimeter, then we vary the oscillator frequency. As the power consumption increases with voltage [16], we keep the voltage to the lowest level required to operate all the modules, which we found to be 2 V. Table 1 demonstrates the power breakdown of both VLMs. The thresholding circuit together with the solar cell consumes 0.5  $\mu$ W of power to sense and digitize shadow events. The Scatterlight mechanism consumes power proportional to the backscatter frequency. The power consumption of Scatterlight varies between 19.5  $\mu$ W to 120  $\mu$ W when the backscatter frequencies are between 100 kHz to 1 MHz. In tVLM,

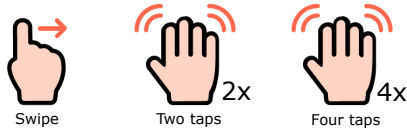


**Figure 7: Supported hand gestures using the tVLM.** We support three hand gestures: Swipe is represented by a single and brief hand movement, Two and Four taps are represented by fixed number of slower palm movements.

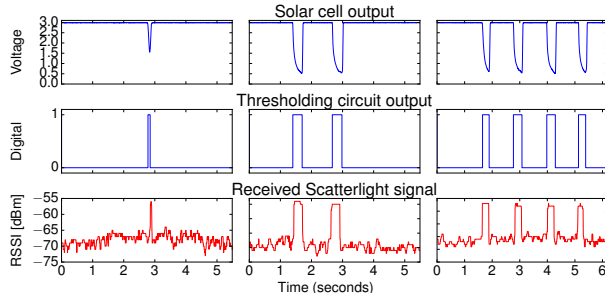


**Figure 8: Sensing hand gestures using tVLM.** We detect three hand gestures (Swipe, Two taps, Four taps) at  $20 \mu\text{W}$ s of power. The top two rows shows output at the tVLM, the bottom row shows received signal at the end-device.

the Scatterlight mechanism is enabled when there is a shadow sensing event, otherwise it consumes  $0.5 \mu\text{W}$  required for the digitization operation. Figure 6 demonstrates the power consumption for the tVLM for different operating frequencies.

**Sensing and communicating gestures.** We investigate the ability of our system to detect hand gestures. Starting with tVLM, we focus on three gestures: swipe, two taps, and four taps. These gestures are illustrated in figure 7. We perform the experiment indoors, and locate the carrier generator source approximately 20 m away from the tVLM. The carrier generator is not in line-of-sight from the receiver. We place the tVLM at a distance of 1 m away from the receiver. Next, we perform hand gestures over the tVLM’s solar cell. We track the digital and analog signal from the VLM, and sample the RSSI at the RF receiver at an interval of 10 ms. Figure 8 shows the distinct patterns caused by the gestures in the received RSSI samples at the CC1310 RF receiver. However, due to the 1-bit digitization performed by the thresholding circuit in VLM 1, it cannot detect less significant variations in the analog signal.

Next, we evaluate the improvement of aVLM over tVLM for gesture detection. For this experiment, we select four gestures that require higher sensing resolution, and thus cannot be detected by the tVLM: push, pull, punch, and block. Push is represented by a decreasing palm movement over the solar cell, and pull is the opposite to push. Punch is a push movement followed by a pull movement. Block is simply a complete obstruction of the solar cell. To perform the experiment, we locate the 2.4 GHz carrier generator 1 m away from the aVLM, and the receiver 3 m away from the receiving SDR. Next, we perform the hand gestures over the aVLM’s solar cell while reconstructing the analog signal at the receiving SDR using equation 2. Figure 9 shows the result after a 6-bit analog conversion at the receiver. Our experiment demonstrates that aVLM is able to detect small variations in light levels due to the gestures.

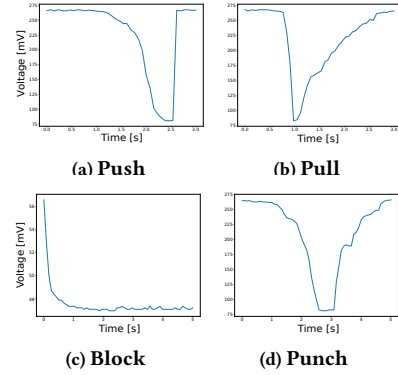


**Figure 9: Sensing hand gestures using aVLM.** Analog backscatter enables us to detect four hand gestures: Push, Pull, Block, and Punch that requires higher sensing resolution. The figures illustrate a 6-bit representation these gestures obtained at the receiver.

## 5 CONCLUSION

In this paper, we presented the first system that uses a solar cell to achieve sub  $\mu\text{W}$  of power to detect shadow events. Further, the system uses a novel mechanism to delegate sensor readings to the end-devices at tens of  $\mu\text{W}$ s of peak power consumption by avoiding energy expensive computational block. Our initial results demonstrate the ability to detect and communicate hand gestures at orders of magnitude lower power consumption when compared to the state-of-the-art systems.

## REFERENCES

- [1] Mohamed Ibrahim et al. 2016. Visible Light Based Activity Sensing Using Ceiling Photosensors. In *VLCS 2016*.
- [2] Bryce Kellogg, Vamsi Talla, Shyamnath Gollakota, and Joshua R Smith. 2016. Passive wi-fi: Bringing low power to wi-fi transmissions. In *USENIX NSDI 2016*.
- [3] Ye-Sheng Kuo et al. 2014. Luxapose: Indoor Positioning with Mobile Phones and Visible Light. In *ACM MOBICOM 2014*.
- [4] Tianxing Li, Chuankai An, Zhao Tian, Andrew T Campbell, and Xia Zhou. 2015. Human sensing using visible light communication. In *ACM MOBICOM 2015*.
- [5] Tianxing Li, Qiang Liu, and Xia Zhou. 2016. Practical human sensing in the light. In *ACM MOBISYS 2016*.
- [6] Tianxing Li, Xi Xiong, Yifei Xie, George Hito, Xing-Dong Yang, and Xia Zhou. 2017. Reconstructing hand poses using visible light. *Proceedings of the ACM on Interactive, Mobile, Wearable and Ubiquitous Technologies* 1, 3 (2017), 71.
- [7] Vincent Liu et al. 2013. Ambient Backscatter: Wireless Communication out of Thin Air. In *ACM SIGCOMM 2013*.
- [8] Saman Naderiparizi et al. 2018. Towards Battery-Free HD Video Streaming. In *NSDI 2018*.
- [9] Ettus Research. 2013. USRP-B200. (2013). [https://www.ettus.com/content/files/b200-b210\\_spec\\_sheet.pdf](https://www.ettus.com/content/files/b200-b210_spec_sheet.pdf)
- [10] Vamsi Talla, Bryce Kellogg, Shyamnath Gollakota, and Joshua R Smith. 2017. Battery-Free Cellphone. In *ACM UBICOMP 2017*.
- [11] Linear Technology. 2005. LTC6906. (2005). <http://www.analog.com/media/en/technical-documentation/data-sheets/6906fc.pdf>
- [12] Ambuj Varshney et al. 2017. LoRea: A Backscatter Architecture that Achieves a Long Communication Range. In *ACM SENSYS 2017*.
- [13] Zixiong Wang, Dobroslav Tsonev, Stefan Videv, and Harald Haas. 2015. On the design of a solar-panel receiver for optical wireless communications with simultaneous energy harvesting. *IEEE JSAC 2015* (2015).
- [14] Chi Zhang and Xinyu Zhang. 2016. LiTell: Robust Indoor Localization Using Unmodified Light Fixtures. In *ACM MOBICOM 2016*.
- [15] Pengyu Zhang et al. 2014. Ekhonet: High speed ultra low-power backscatter for next generation sensors. In *ACM MOBICOM 2014*.
- [16] Pengyu Zhang et al. 2016. Enabling practical backscatter communication for on-body sensors. In *ACM SIGCOMM 2016*.
- [17] Shilin Zhu et al. 2017. Enabling High-Precision Visible Light Localization in Today’s Buildings. In *ACM MOBISYS 2017*.